



# Analysis and Modeling of Protection System Hidden Failures and Its Impact on Power System Cascading Events

Diptak Pal<sup>1</sup> · Balimidi Mallikarjuna<sup>1</sup>  · M. Jaya Bharata Reddy<sup>1</sup> · D. K. Mohanta<sup>2</sup>

Received: 9 September 2018 / Revised: 17 December 2018 / Accepted: 21 January 2019 / Published online: 1 February 2019  
© Brazilian Society for Automatics--SBA 2019

## Abstract

In this paper, a detailed study of the modes of hidden failures (HFs) in protection systems is carried out, and probabilistic modeling methodology is used for analyzing the impact of HFs on the power system cascading events. Further, the probabilistic model of HFs based on impedance and line power flow is hypothesized for qualitative evaluation of HF's impact on power system cascading disruptions. Numerous case studies have been carried out on the IEEE-118 bus system to assess the effect of HFs by fitting the probability model of line outage based on impedance and power flow. This analysis has successfully identified the most sensitive transmission lines in the network which are having the highest tendency to trip in case of protective system HFs. Also, it has been shown that the probability of major blackouts will be reduced to a more significant extent if the self-checking and monitoring features are incorporated into digital relays. The qualitative analysis of protection system HFs could be helpful in planning, service and maintenance scheduling of a power system as well as determining the locations where an investment warrants the protection system reliability.

**Keywords** Protection system · Hidden failures (HF) · Probabilistic models · Protection system reliability · Power system cascading events

## 1 Introduction

Typically, the parameters of the power system such as power flow through the lines, impedances observed at each end of the lines, and bus voltages are mainly get affected during power system stressed condition. Under such circumstances, the protection system employed for the protection of a large interconnected power system might have some tendency toward incorrect or inappropriate tripping of a circuit

element due to some failures which are undetected under normal operating condition. Such an incorrect and inappropriate operation of the relays can initiate cascaded tripping of circuit elements which ultimately results in catastrophic failures, i.e., blackouts. Few of such kinds are illustrated by reporting some real-time events that occurred previously in some of the massive power grids across the globe. They are

1. August 14, 2003, power outage in North America (NERC Actions on [2003](#) blackout, 2004)
2. Blackout in the European interconnected power grid on November 4, 2006 (Li et al. [2007](#)).
3. The major power outage in India on July 30–31, 2012 (Lai et al. [2013](#)).

The NERC report on significant disruptions occurred in the period from 1984 to 1988 (NERC Disturbance Reports 1984–1988, [1988](#)) is summarized in Tamronglak et al. [1996](#). It has revealed that 73.5% of significant disruptions are because of protective relays' involvement in one way or another way. Also, the studies and investigations on significant blackouts at the USA and Canada in 2003 (Final Report on [2003](#), 2004) and India in 2012 (Final Report on [2012](#)

---

✉ Balimidi Mallikarjuna  
arjun.malli4@gmail.com

Diptak Pal  
diptakpal@gmail.com

M. Jaya Bharata Reddy  
jayabharat\_res@yahoo.co.in

D. K. Mohanta  
dkmohanta@bitmesra.ac.in

<sup>1</sup> Department of Electrical and Electronics Engineering,  
National Institute of Technology, Tiruchirappalli,  
Tamil Nadu, India

<sup>2</sup> Department of Electrical and Electronics Engineering, Birlal  
Institute of Technology, Mesra, Ranchi, India

blackout, 2012) revealed that the protective relays had made a significant contribution to the propagation of cascading failures which ultimately led to the catastrophic failure. A common point observed is that the relay had an undetected defect(s) or HF(s) that were uncovered by the circumstances originated from the other disruptions. Thus, the relay with HFs (faulty relay) can cause a false trip which exacerbates the situation further if a fault is present in adjacent sections of the power system, reverse power flows, or overload of the power system. In other words, the protection device's HFs can cause multiple contingencies, which results in catastrophic disruptions. However, the effect of malfunction of the protection device (due to HFs) on overall system reliability has not been studied well. Usually, the existing protection system is biased toward increased dependability, at the cost of security of the system. Thus, the total system integrity is undermined due to highly redundant local protection schemes. To perform a quantitative analysis of HFs, few methods which had been proposed previously are discussed in detail as follows.

Analysis of cascading scenarios using simulations can be daunting because such rare situations are difficult to capture in large but limited databases. The conventional techniques cannot be utilized reasonably to find the probability of occurrence of the major disturbances, though thousands of load flows or transient stability cases can be involved in a database. Further, accurate detection of HFs in a protective relay is a vital aspect of enhancing the security of the protective system (Zhao et al. 2015). Analysis and modeling of the characteristics and harmfulness of HFs can help in designing robust protection system (Gao et al. 2013). Advanced protective relays with self-monitoring aided with communication network can assist in detecting the presence of HFs and mitigating the impact of HFs (Horowitz et al. 1995). The authors of Thorp et al. 1998; Bae and Thorp 1999 have proposed methodologies based on importance sampling method. In importance sampling, the simulations are performed with altered probabilities which make the unlikely events more likely and the correct answers are obtained by processing the simulation results. Later, a cascade model was proposed (Dobson et al. 2002) to analyze the impact of the HF. The model had been used to examine the criticality of blackouts under the situation of random overloading of transmission lines and multiple contingencies. Another methodology based on coupled map lattices was introduced by Wang and Xu (2004) for investigating cascading failures. It was found that in small-world and scale-free coupled map lattices, the occurrence of the cascading failures is much easier than in globally coupled map lattices.

Furthermore, Wu et al. (2006) have studied the cascading failures in scale-free networks with community structure, and simulations are carried out for cascade propagation of such systems with different modularity parameters. It was

observed that triggering of cascading failures in the network with small modularity is much easier than that of the larger one. Besides, a new parameter known as power flow entropy had been introduced for analyzing cascading failures in power systems. Various risk assessment methodologies (Hui et al. 2012) and early warning mechanism (Qi et al. 2016) were developed using power flow entropy and have produced satisfactory results. Also, recently, artificial intelligence has also been used for investigating catastrophic failures in the power grid. An enhanced cascading failure model was proposed in Sun et al. 2017, integrating data mining techniques to simulate the process of cascading failure propagation in better way. However, the above research studies have not discussed adequately regarding methodologies to prevent cascading failures and blackouts. The authors of Seyed and Sanaye-Pasand 2009; Aghamohammadi and Salimian 2018 discussed the load shedding is one of the methods to avoid blackouts. However, the analysis is not from the point of view of propagation of cascading failures. Albinali and Meliopoulos (2017) have developed a new centralized substation monitoring scheme which identifies the HFs using real-time dynamic state estimation. The proposed scheme performs a hypothesis test to distinguish the contingencies as HFs or power faults. The proposed architecture can be employed for reliable data management at the substation along with optimization of communication system requirement within the substation. Furthermore, Jiao et al. (2018) have proposed HF detection method which employs the features of protection systems obtained from the records of a sequence of multiple events under disturbances and faulty conditions.

The previous studies have indicated that the protection system HFs play a significant role in the succession of events that result in power system disruptions and major blackouts. However, very few qualitative evaluations were done before for analyzing such impacts of HFs in the protection system. In this paper, various modes of HFs, which are considered as one of the most contributing factors for the propagation of cascading failures leading to blackouts, are studied in detail. Furthermore, probabilistic/statistical modeling technique (Chen et al. 2005; Henneaux 2015) has been adopted for analyzing the impact of cascading failures in a power system. The test cases considered are simulated on the IEEE-118 bus system. MATLAB software (2014a) has been utilized for validating the proposed methodology. The results obtained through rigorous simulations using MATLAB script have shown that the chances of major blackouts will be reduced to a greater extent due to HFs if the self-monitoring and self-checking features are incorporated into digital relaying. This valuable information could be helpful in areas such as planning, service and maintenance scheduling of a power system as well as determining the locations where an investment warrants the protection system reliability.

## 2 Probabilistic Modeling of Hidden Failures

In this section, the probabilistic modeling of HFs is discussed in detail. The NERC report (NERC Disturbance Reports 1984–1988, 1988) reveals that the most significant disruptions generally involve a number of improbable (should not have happened) events. It is challenging to perform simulation studies for capturing a number of low-probability events. Almost few attempts have been made to simulate the temporal spreading of the disruptions since the exact probabilities of the various improbable events are not well known. So, in this section, a technique has been established for estimating the probability of cascading disruptions in terms of the individual probabilities of protective relay HFs which are leading to an incorrect trip. The conclusion is not dependent on the exact numbers used for the probability that an exposed line will trip because the individual probabilities are treated parametrically. A probability model has been hypothesized for the existence of HFs in the overall line protection. The assumption is that if any line is sharing a bus with a given transmission line ‘*L*’ trips, then the HFs in the protective system of the line ‘*L*’ are exposed. That is, there is a probability ‘*p*’ that the line ‘*L*’ will trip. A four-bus power system is considered as shown in Fig. 1 to illustrate the phenomenon of cascaded tripping of transmission lines due to HFs in the protection system.

One-line tripping due to a sustained fault may result in incorrect tripping of all the lines connected to its ends due to the presence of the protection system HFs. The probability of such tripping is quite small. For example, assume that line L4 is tripped legitimately; then, lines L1, L2, L3, and L5 are exposed to false tripping because of HFs in the relays

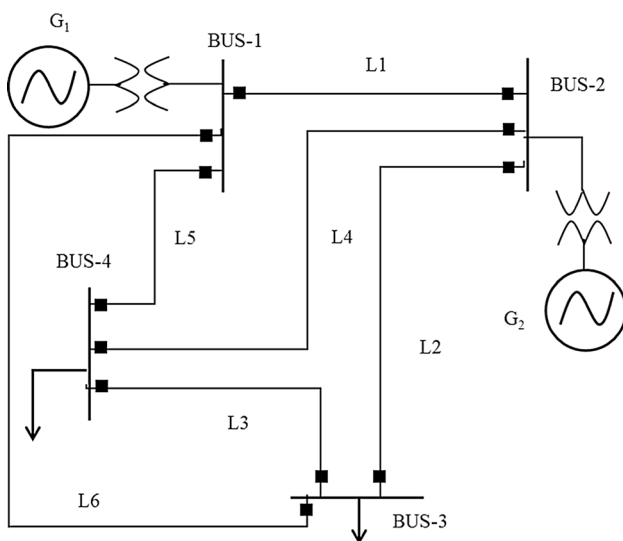


Fig. 1 One-line diagram of a four-bus system (Bae and Thorp 1999)

protecting them. Line L6 is not exposed since it has not been connected to either Bus-2 or Bus-4. Further, assume that the probability of tripping and not tripping of an exposed line by corresponding protective devices is taken as a constant ‘*p*’ and ‘*q*’ ( $= 1 - p$ ), respectively. Consider a condition for a ‘significant power system disruption.’ In other words, at least one bus has no lines connected. This is an unrealistic condition for a large system. However, it is quite adequate to illustrate for a small system (Fig. 1). The overall probability of the ‘significant power system disruption’ initiated by the loss of a line due to protective device malfunction is estimated using Eq. 1. Equation 1 can be written as a 12th-order polynomial in ‘*p*’ if ‘*q*’ is replaced with  $(1 - p)$ . It is represented in Fig. 2 against the probability of HF (*p*).

$$P_a = p^4 + 4p^3q + 2p^2q^2 + 2p^2q^2[2 - q^4 - q^6(1 + 2p + p^2) + 4p^2q^2[p^2q + 3pq^2 + q^3(2 - 2q^3 - pq^4)]] \quad (1)$$

where  $P_a$  is the overall probability of a major disturbance and *p* the probability of line tripping incorrectly due to HF.

In the above analysis of cascading events and significant disruptions due to HFs of protective relays in transmission lines, the probability of transmission line tripping incorrectly is taken as constant. However, in contradiction to the above analysis, for analyzing the cascaded tripping of transmission lines the value of probability (*p*) of individual line tripping has been considered as a variable rather than the fixed value ‘*p*.’ Thus, each line will have different probabilities of tripping incorrectly in a more general problem.

The implementation of probabilistic modeling methodology of HFs in the protection system to evaluate its impact on power system cascading events is discussed here. Thus, the probabilistic modeling of HFs in power protection system is totally based on hypothesis including load/generation variation. Two types of modeling strategy, one based on impedance of a relay (impedance-based HF model) and the other based on line power flow (line power flow-based model of

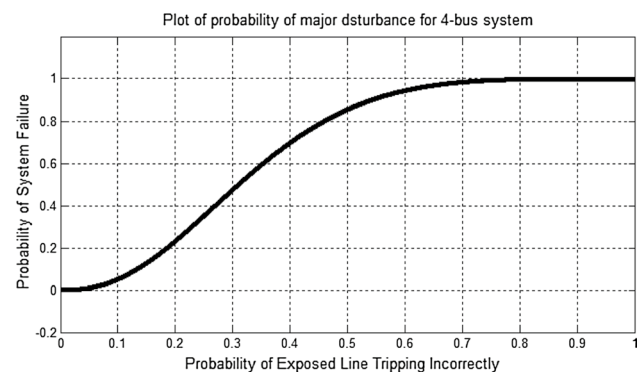


Fig. 2 Probability of major disruptions for the four-bus system shown in Fig. 1

HFs), have been used to show that the results obtained are consistent. Practically, both the methods are identical. Since the study depends on the concept of probability, the two different methods are necessary to validate the results obtained from two identical kinds of models. The following subsection illustrates the models of HFs based on the impedance observed by a relay and the line power flows.

## 2.1 Impedance-Based Hidden Failure Model

In this subsection, the probability of incorrect tripping of an exposed line is modeled as a function of the impedance of the line protection relay shown in Fig. 3a. So, in order to account for the fault detector value, a value of three times the Zone-1 impedance ( $Z-3$ ) of the relay is selected with the assumption that if the impedance of the relay is less than  $Z-3$ , then the probability of incorrect tripping due to HF will get magnified. Where the probability decreases exponentially as the apparent impedance of the relay goes beyond  $Z-3$ . In Fig. 3a, the value of ' $p$ ' is chosen by hypothetically by making a rough idea of the risk associated with HF in a protective relay. The value of ' $p$ ' is changed sometimes in simulations to show the reduction in the probability of major

disturbance in case the probability of HF is reduced by 50%. The exponential part of Fig. 3a is fitted using Eq. 2.

$$P_a = p * e^{(-Z/(Z-3))} \quad (2)$$

where  $Z$  is the impedance observed by the relay and  $Z-3$  the value of three times the Zone-1 setting.

## 2.2 Line Power Flow-Based Model of HFs

The line outage model based on power flow through lines has also been utilized for carrying out the simulation studies of cascading disturbances due to HF. The line outage model is shown in Fig. 3b. In this figure, the linear portion of the curve is fitted using the expression shown in Eq. 3.

$$P_a = \frac{1-p}{P_{\max} - P_{\max}^{\text{normal}}} \times P + \frac{p \times P_{\max} - P_{\max}^{\text{normal}}}{P_{\max} - P_{\max}^{\text{normal}}} \quad (3)$$

where  $P$  shown in Fig. 3b is power flow through the line;  $P_{\max}$  is the maximum withstanding capacity of power flow through the transmission line;  $P_{\max}^{\text{normal}}$  is the maximum value of normal power flow through the line.

The value of  $1.5 \times P_{\max}$  is considered as an upper threshold which can be related to the thermal limit of the line in real power system scenario. Since the probability model related to line flows is totally based on the hypothetical concept, a value of 1.5 times the maximum power flow through the transmission lines is selected. The steady-state angular stability limit governs the value of  $P_{\max}$  ( $P_{\max} = (|V1| \times |V2|)/X$ ), whereas the value  $1.5 \times P_{\max}$  is chosen to have the upper limit based on thermal rating of the transmission lines. In a practical scenario, the value of  $1.5 \times P_{\max}$  can change for different transmission lines.

## 3 Probabilistic Methodology

In this section, a technique for determining the probability of cascading disruptions regarding the individual probabilities of an HF in a protective relay which may result in an incorrect trip has been discussed. The conclusion is not dependent on the exact numbers used for the probability that an exposed line will get tripped. It is because the individual probabilities are treated parametrically and the power system protection is designed accordingly (Tamronglak et al. 1996). A probability model has been hypothesized for the existence of HFs in the overall transmission line protection. It is assumed that if any line is sharing a bus with a given transmission line ' $L$ ' trips, then the HFs in the line  $L$  are exposed. Specifically, there is a probability ' $p$ ' that the line  $L$  will trip.

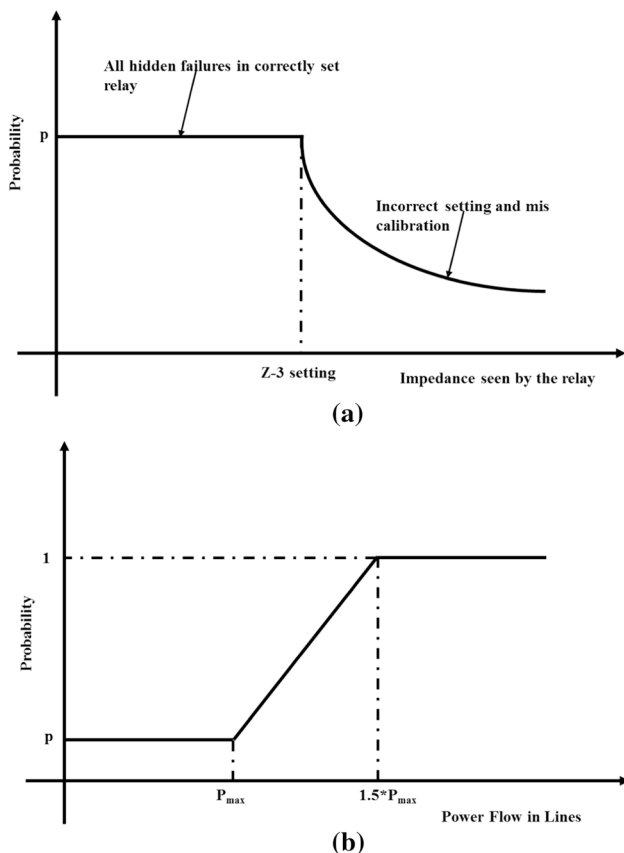


**Fig. 3** a Impedance-based probability model of exposed line tripping incorrectly, b line power flow-based probability model of line outage

The steps involved in the proposed methodology, shown in Fig. 4, for simulating the rare power system cascading disruptions are presented as follows:

- Step 1:** Read the line and bus data of a test power system.  
**Step 2:** Perform the load flow analysis using the Newton–Raphson (NR) method to find the steady-state voltage and angles.  
**Step 3:** Select the transmission line for the initial tripping event.  
**Step 4:** Modify the Y-bus matrix, perform load flow analysis, and determine the exposed line  
**Step 5:** Calculate the probability ( $P_{HF}$ ) of the false tripping of exposed lines based on the line outage.  
**Step 6:** Execute the random tripping on the exposed line with  $P_{HF}$  is greater than the randomly generated number.  
**Step 7:** Record a variable ( $T_k$ ).

$$T_k = \sum_{i=1}^{\text{no. of lines tripped}} \log_e (P_{HF}) + \sum_{i=1}^{\text{no. of lines tripped}} \log_e (1 - P_{HF}) \quad (4)$$

**Step 8:** Read all the lines that are tripped.

**Step 9:** If load flow is not converging or all the line connected to a bus are tripped, then got to Step 10. Else

$$(Y_{Bus})_{New} = (Y_{Bus})_{Old} \quad (5)$$

and go to Step 4.

**Step 10:** Record a variable  $P_j$

$$P_j = \sum_{k=1}^{\text{no. of steps}} \log_e (T_k). \quad (6)$$

**Step 11:** If number of iterations are equal to 3000, then stop; else, go to Step 2.

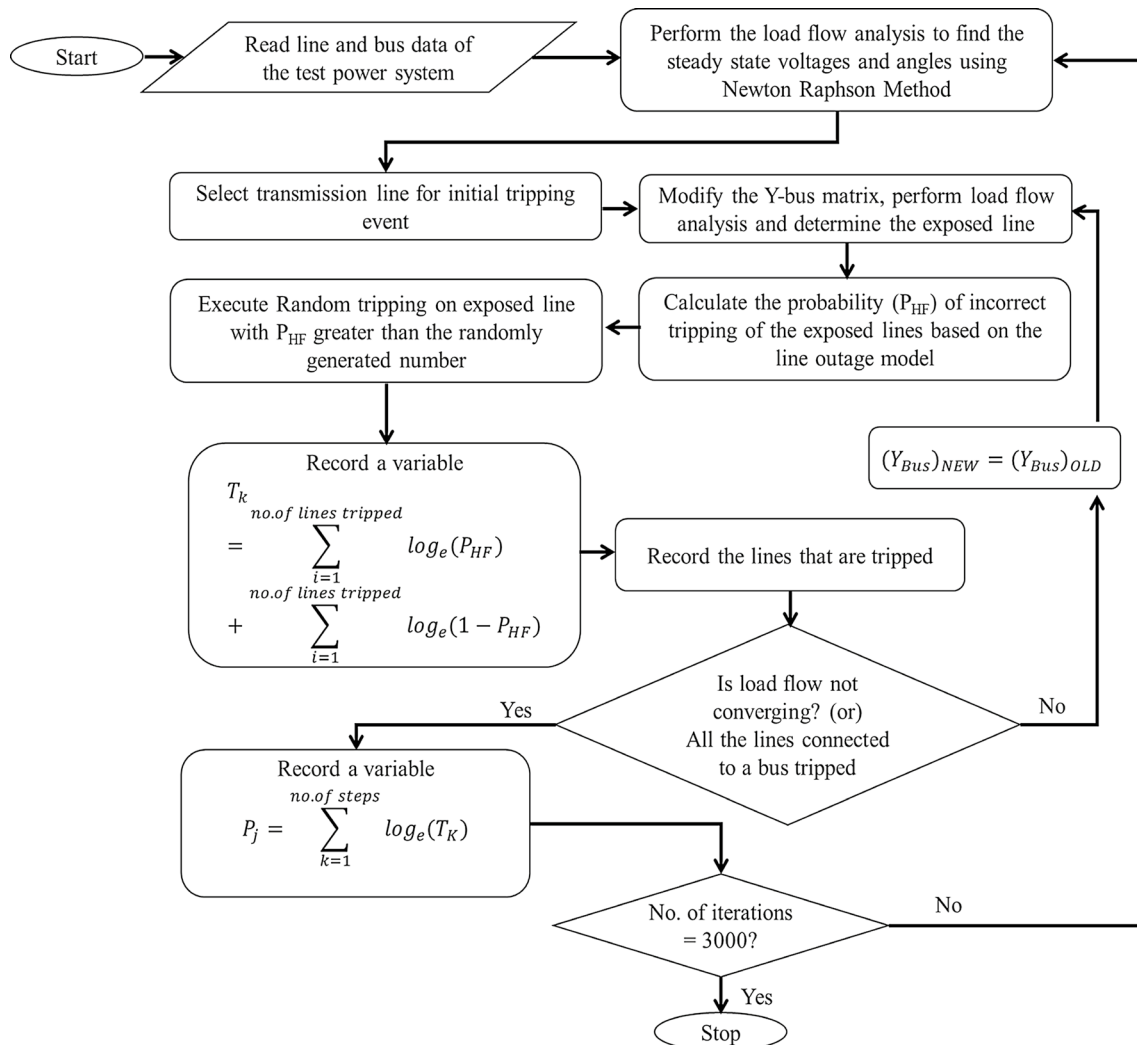


**Fig. 4** Flowchart of the proposed methodology for estimation of the probability of major disruptions due to HF



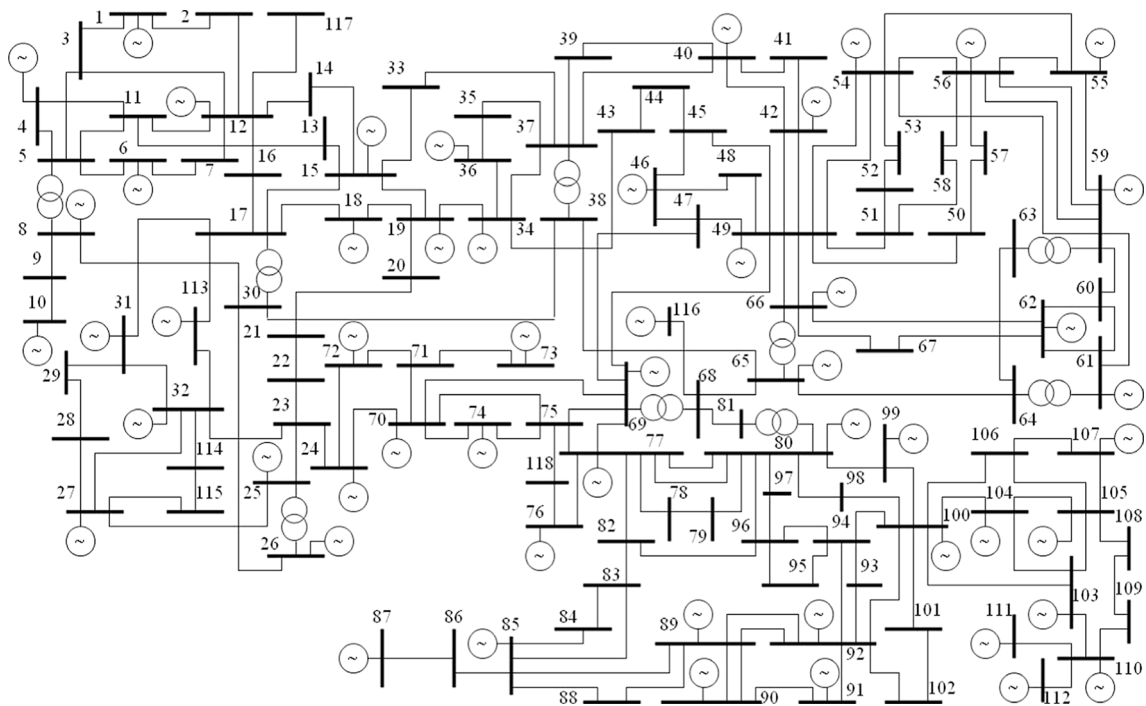


**Fig. 5** Single-line diagram of the IEEE-118 bus system

## 4 Results and Discussions

Previously, little simulation work has been done in the area of cascading disruptions of the bulk power system regardless of the apparent importance to the industry. The reasons are the enormous complexity associated with it. The difficulty associated with the simulation of rare events coupled with the lack of data on which the base models depend on has precluded the work in the area. For validating the proposed methodology to simulate such unlikely events, the IEEE-118 bus system shown in Fig. 5 is a consideration. The initial step for the simulation study is to perform NR load flow analysis on the system considered. So, in line with the steps of the simulation, load flow analysis is done on the IEEE-118 bus system. The results obtained from load flow analysis are shown in Figs. 6, 7, and 8. Figure 6 shows the magnitudes of steady-state bus voltages obtained after performing NR load flow analysis. Figure 7 shows the steady-state angle of bus voltage for all the 118 buses. Figure 8 shows the real power injections at each bus. These results are necessary for subsequent steps of simulations since the bus voltage magnitudes and angles along with real power injections at each bus can be utilized for calculating the impedance of the relays and also the power flow through the lines. The line current can be calculated by utilizing the  $Y$ -bus matrix obtained from the line data of the IEEE-118 bus system and the bus voltage magnitudes and angles. Furthermore, for carrying out

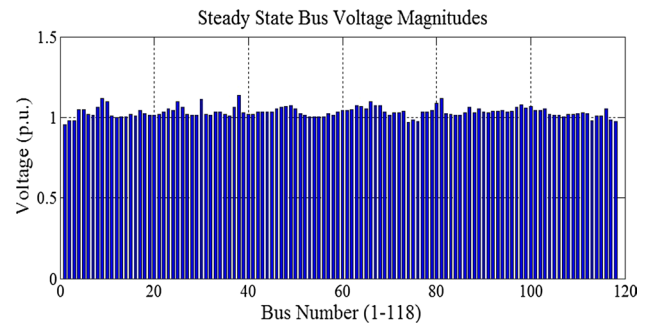


**Fig. 6** Magnitudes of steady-state bus voltages (p.u.) in IEEE-118 bus system

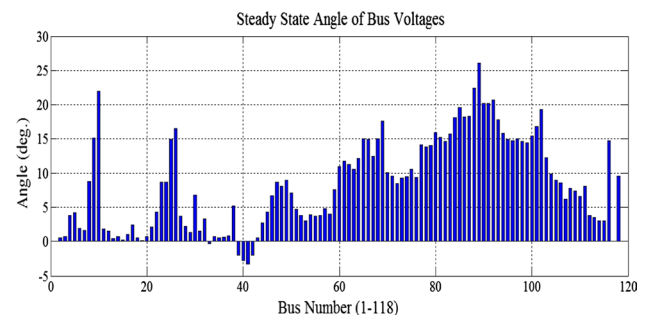


**Fig. 7** Angles of steady-state bus voltages in the IEEE-118 bus system

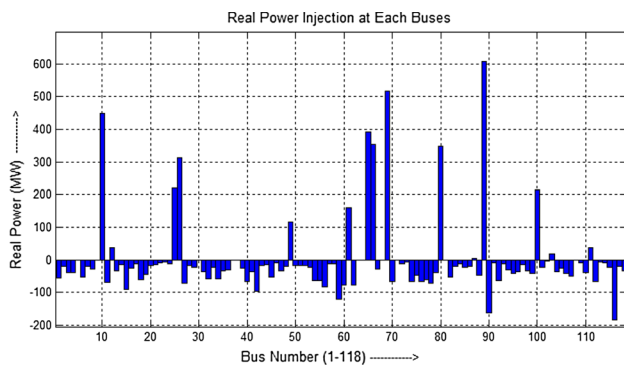


**Fig. 8** Real power injections at each bus in the IEEE-118 bus system

various case studies on the IEEE-118 bus system, ‘ $p$ ’ is taken as a function of impedance of the relay with a lower probability if the impedance is large and also a function of power flow through the lines with a higher probability if the line power flow is large.

**Table 1** Sample paths and probabilities for cascading failures for initial tripping of line 11–12 with  $p=0.1$

S. no.	Tripped lines	Probability
1.	11–12, 12–2, 2–1	$2.77 \times 10^{-06}$
2.	11–12, 12–2, 2–1	$7.84 \times 10^{-06}$
3.	11–12, 11–4, 11–5, 5–4	$6.48 \times 10^{-07}$
4.	11–12, 11–4, 11–5, 5–8, 5–4	$9.89 \times 10^{-08}$
5.	11–12, 11–13, 11–5, 5–8, 8–9, 9–10	$9.58 \times 10^{-10}$
6.	11–12, 11–4, 11–5, 5–6, 5–3, 3–1, 1–2	$1.04 \times 10^{-11}$
7.	11–12, 12–2, 12–3, 3–1, 3–5	$3.13 \times 10^{-11}$
8.	11–12, 12–7, 12–2, 12–3, 3–1, 3–5	$2.14 \times 10^{-12}$
9.	11–12, 12–2, 12–3, 12–7, 12–117	$9.89 \times 10^{-13}$
10.	11–12, 12–2, 12–7, 12–3, 3–5, 5–8, 5–11, 11–4, 11–13	$4.44 \times 10^{-16}$
11.	11–12, 12–7, 12–2, 12–3, 3–5, 5–8, 5–11, 5–6, 5–4	$1.48 \times 10^{-18}$

**Table 2** Sample paths and probabilities for cascading failures for initial tripping of line 37–40 with  $p=0.1$

S. no.	TRIPPED lines	Probability
1.	37–40, 37–34, 37–38, 38–65, 38–30	$1.16 \times 10^{-06}$
2.	37–40, 37–38, 38–65, 38–30, 65–66	$1.71 \times 10^{-07}$
3.	37–40, 37–38, 38–30, 30–8, 8–5, 8–9	$1.885 \times 10^{-08}$
4.	37–40, 37–39, 37–34, 37–35, 37–38, 37–33	$2.32 \times 10^{-09}$
5.	37–40, 37–34, 37–38, 37–39, 37–35, 35–36	$7.95 \times 10^{-10}$
6.	37–40, 37–34, 37–39, 37–38, 38–65, 38–30, 38–30, 65–64	$1.48 \times 10^{-11}$
7.	37–40, 37–38, 37–34, 34–19, 19–18, 34–36, 34–43	$1.82 \times 10^{-12}$
8.	37–40, 37–34, 37–39, 37–35, 37–38, 38–65, 65–68, 68–116	$2.18 \times 10^{-13}$
9.	37–40, 37–34, 37–39, 37–38, 38–65, 65–68, 65–64, 65–66	$8.96 \times 10^{-14}$
10.	37–40, 37–38, 38–30, 30–17, 17–15, 17–113, 17–18, 17–16, 17–31	$1.49 \times 10^{-15}$
11.	37–40, 37–35, 37–34, 34–19, 19–15, 15–13, 15–17, 17–31, 17–18, 17–113, 17–16, 17–30	$1.26 \times 10^{-16}$
12.	37–40, 37–34, 37–35, 37–38, 38–30, 30–26, 30–17, 17–15, 17–18, 15–33, 15–13, 15–14, 15–19	$1.53 \times 10^{-19}$
13.	37–40, 40–39, 40–42, 42–49, 49–51, 49–54, 54–56, 56–59, 56–57, 59–63, 59–60, 59–61, 61–60, 60–62	$5.4 \times 10^{-24}$

#### 4.1 Simulation of Cascading Events using Impedance-Based Model of Hidden Failure

The simulation is performed after conducting the NR load flow analysis by considering an initial line tripping as the initiating event, which leads to propagation of cascading failures of protection system ultimately resulting in black-outs as per the proposed algorithm presented in Sect. 3. In this paper, each line tripping is studied as individual case. Several cases are considered with different line tripping as the initiating events and results are tabulated in Tables 1, 2, 3, 4, 5, 6, 7, and 8.

The line connected between Bus-11 and Bus-12, as shown in Fig. 5, legitimate tripping is considered as the first case. The sequence of events (sample paths) of tripping of various transmission lines along with the probabilities of a different sequence of tripping events obtained through the simulation is tabulated in Table 1.

The first and second rows of Table 1 show the same sample paths, but the probability values are different. The

**Table 3** Sample paths and probabilities for cascading failures for initial tripping of line 56–59 with  $p=0.1$ 

S. no.	Tripped lines	Probability
1.	54–56, 56–59, 59–63, 63–64	$5.6 \times 10^{-06}$
2.	54–56, 56–59, 59–55, 55–54, 55–56	$2.08 \times 10^{-08}$
3.	54–56, 54–49, 49–66, 66–65, 66–67, 66–62	$1.76 \times 10^{-10}$
4.	54–56, 54–49, 49–66, 66–65, 65–64, 65–68, 68–116	$6.34 \times 10^{-11}$
5.	54–56, 56–59, 59–63, 59–60, 60–61, 61–59, 61–64, 61–62	$8.17 \times 10^{-14}$
6.	54–56, 54–49, 54–55, 55–59, 59–54, 59–56, 59–63, 63–64	$3.11 \times 10^{-17}$
7.	54–56, 54–49, 49–66, 49–51, 49–50, 49–42, 49–45, 49–48, 49–47, 47–69, 69–49	$4.25 \times 10^{-19}$
8.	54–56, 56–59, 59–60, 59–63, 59–61, 61–64, 61–62, 62–66, 62–60, 62–67	$6.48 \times 10^{-20}$
9.	54–56, 54–49, 49–66, 49–47, 47–69, 69–49, 69–68, 69–70, 70–75, 75–74, 75–77, 75–69, 69–77	$1.02 \times 10^{-22}$
10.	54–56, 56–59, 56–55, 55–59, 59–54, 59–63, 59–60, 60–61, 61–62, 61–64, 64–63, 64–65	$9.39 \times 10^{-24}$
11.	54–56, 56–57, 56–59, 59–54, 54–49, 59–63, 59–61, 59–60, 60–62, 62–66, 66–49, 49–47, 66–65, 65–64, 65–68, 68–69, 69–47, 69–70, 70–71, 69–77, 77–76, 76–118	$1.02 \times 10^{-31}$
12.	54–56, 56–59, 59–63, 59–55, 59–54, 54–49, 49–42, 49–66, 49–69, 69–70, 69–77, 77–80, 77–76, 77–75, 75–118, 75–74, 75–70, 70–71, 70–24, 24–23, 23–22, 23–32, 32–113, 32–17	$9.79 \times 10^{-39}$

**Table 4** Sample paths and probabilities for cascading failures for initial tripping of line 69–75 with  $p=0.1$ 

S. no.	Tripped lines	Probability
1.	69–75, 69–68, 68–116	$4.65 \times 10^{-04}$
2.	69–75, 69–47, 69–68, 68–116	$3.95 \times 10^{-06}$
3.	69–75, 69–49, 69–77, 69–68, 68–116	$1.14 \times 10^{-08}$
4.	69–75, 75–77, 77–80, 80–79, 79–78	$1.46 \times 10^{-09}$
5.	69–75, 69–47, 69–70, 69–68, 69–77, 69–48	$9.81 \times 10^{-11}$
6.	69–75, 69–70, 69–77, 69–68, 68–65, 68–81, 68–116	$1.64 \times 10^{-12}$
7.	69–75, 69–70, 69–49, 49–66, 66–65, 65–38, 65–64, 65–68	$1.27 \times 10^{-15}$
8.	69–75, 75–77, 77–80, 77–69, 69–68, 77–78, 77–82, 77–77	$6.1 \times 10^{-16}$
9.	69–75, 69–70, 69–77, 69–47, 69–68, 68–65, 65–64, 65–66, 65–38	$9.23 \times 10^{-18}$
10.	69–75, 69–77, 69–68, 69–70, 70–71, 70–24, 24–23, 23–25, 25–26, 25–27	$1.96 \times 10^{-20}$
11.	69–75, 69–47, 69–70, 69–68, 69–77, 77–82, 77–78, 77–75, 77–80, 80–79, 80–81, 81–68	$1.05 \times 10^{-23}$
12.	69–75, 69–68, 69–70, 69–77, 69–49, 49–42, 49–54, 54–56, 56–58, 56–57, 56–59, 56–60, 59–55, 59–54, 59–61, 59–64, 61–64, 64–63, 63–59	$1.19 \times 10^{-33}$

**Table 5** Sample paths and probabilities for cascading failures for initial tripping of line 11–12 with  $p=0.05$ 

S. no.	Tripped lines	Probability
1.	11–12, 11–13, 13–15	$2.75 \times 10^{-06}$
2.	11–12, 11–5, 11–4, 4–5, 11–13	$1.8 \times 10^{-08}$
3.	11–12, 11–13, 11–4, 4–5	$1.87 \times 10^{-11}$
4.	11–12, 12–2, 12–3, 3–1, 3–5	$1.82 \times 10^{-11}$
5.	11–12, 11–5, 5–3, 5–8, 8–9, 8–30	$4.9110^{-12}$
6.	11–12, 12–2, 12–14, 12–7, 7–6	$3.1 \times 10^{-15}$
7.	11–12, 12–7, 12–2, 12–3, 3–5, 5–8, 5–4, 8–30, 30–38, 30–26, 26–25	$1.5 \times 10^{-23}$

reason is the difference in tripping sequence; for example, initially the line 11–12 is tripped legitimately. However, in the sequential steps, either one of the lines 11–2 and 2–1 or both the lines 11–2 and 2–1 have tripped simultaneously resulting in different numerical values of probabilities. The probability of the major disruption initiated with an 11–12 trip is calculated by summing all the probabilities of sample paths obtained through the simulation studies. For the case shown in Table 1, the probability of major disruption ( $P_a$ ) is found to be  $1.14 \times 10^{-5}$ , when the number of simulation steps ' $N$ ' and the probability of individual line incorrect tripping are 3000 and  $p=0.1$ , respectively.

A similar kind of simulations is performed with different initiation line tripping (37–40, 56–59, and 69–75 separately) for the same number of iterations and probability of individual line incorrect tripping as above. The sample paths of



**Table 6** Sample paths and probabilities for cascading failures for initial tripping of line 37–40 with  $p=0.05$ 

S. no.	Tripped lines	Probability
1.	37–40, 40–39, 39–37	$4.99 \times 10^{-06}$
2.	37–40, 37–34, 34–36, 36–35	$1.02 \times 10^{-07}$
3.	37–40, 37–38, 38–30, 30–17, 30–8, 30–26	$3.31 \times 10^{-08}$
4.	37–40, 37–38, 37–33, 37–34, 37–35, 37–39	$4.36 \times 10^{-09}$
5.	37–40, 37–35, 37–34, 37–38, 38–30, 38–65	$3.79 \times 10^{-10}$
6.	37–40, 37–39, 37–35, 37–38, 37–34, 37–33	$6.31 \times 10^{-11}$
7.	37–40, 37–35, 37–38, 38–30, 30–17, 30–26, 30–8	$1.12 \times 10^{-12}$
8.	37–40, 37–35, 37–38, 37–33, 37–34, 34–19, 34–36, 34–43	$1.69 \times 10^{-14}$
9.	37–40, 37–38, 38–65, 65–66, 66–49, 66–62, 62–61, 66–67	$3.2 \times 10^{-14}$
10.	37–40, 37–38, 37–39, 38–65, 65–64, 65–66, 66–49, 66–67, 66–62	$1.98 \times 10^{-17}$
11.	37–40, 37–38, 38–65, 65–66, 66–49, 49–69, 69–75, 69–68, 68–81, 68–116	$5.57 \times 10^{-19}$
12.	37–40, 40–39, 40–42, 42–49, 49–66, 49–51, 49–69, 49–48, 69–68, 68–65, 68–118	$5.2 \times 10^{-22}$
13.	37–40, 37–35, 37–38, 38–30, 30–17, 17–16, 17–113, 17–31, 17–15, 15–13, 15–19, 19–18, 19–34, 34–37, 37–33, 37–39	$1.13 \times 10^{-34}$

**Table 7** Sample paths and probabilities for cascading failures for initial tripping of line 56–59 with  $p=0.05$ 

S. no.	Tripped lines	Probability
1.	56–59, 59–63, 63–64	$6.71 \times 10^{-07}$
2.	56–59, 56–54, 56–57, 56–58, 56–55	$1.12 \times 10^{-09}$
3.	56–59, 56–54, 54–55, 55–59, 55–56	$1.82 \times 10^{-09}$
4.	56–59, 59–63, 59–61, 61–60, 61–62, 61–64	$1 \times 10^{-10}$
5.	56–59, 56–54, 54–55, 55–59, 59–63, 63–64	$4.24 \times 10^{-11}$
6.	56–59, 56–54, 56–55, 55–59, 59–63, 63–64	$5.66 \times 10^{-12}$
7.	56–59, 59–63, 59–60, 59–61, 61–62, 61–60, 60–62	$8.08 \times 10^{-14}$
8.	56–59, 59–55, 59–63, 59–61, 61–60, 60–62, 61–64, 64–63	$4.16 \times 10^{-14}$
9.	56–59, 56–54, 54–49, 54–55, 54–59, 59–61, 59–55, 59–63, 59–60	$1.82 \times 10^{-20}$
10.	56–59, 59–54, 54–56, 54–49, 49–42, 49–66, 66–65, 65–38, 65–64, 64–61, 64–63	$1.25 \times 10^{-21}$
11.	56–59, 56–54, 54–49, 49–50, 49–66, 66–65, 65–38, 38–30, 30–8, 30–17, 17–31, 17–113, 17–16, 17–18, 17–15	$3.5 \times 10^{-30}$
12.	56–59, 59–54, 54–56, 54–55, 54–49, 49–42, 49–48, 49–50, 49–51, 49–45, 49–69, 69–75, 75–74, 75–77, 77–76, 76–118	$9.82 \times 10^{-35}$

**Table 8** Sample paths and probabilities for cascading failures for initial tripping of line 69–75 with  $p=0.05$ 

S. no.	Tripped lines	Probability
1.	69–75, 69–68, 68–116	$4.94 \times 10^{-03}$
2.	69–75, 69–70, 69–68, 68–116	$1.32 \times 10^{-05}$
3.	69–75, 69–70, 69–68, 68–81, 68–116	$4.45 \times 10^{-07}$
4.	69–75, 69–68, 69–77, 69–70, 69–47, 69–49	$2.52 \times 10^{-18}$
5.	69–75, 69–47, 69–49, 69–77, 69–68, 69–70, 77–75	$2.46 \times 10^{-10}$
6.	69–75, 69–70, 69–77, 77–75, 75–70, 75–74, 74–70	$2.36 \times 10^{-12}$
7.	69–75, 69–68, 69–77, 69–49, 69–70, 70–75, 75–77, 75–118, 75–74	$4.74 \times 10^{-14}$
8.	69–75, 75–77, 77–76, 77–80, 80–81, 80–79, 80–97, 80–96, 80–99, 99–100	$1.36 \times 10^{-16}$
9.	69–75, 69–49, 69–68, 68–65, 69–70, 69–77, 77–80, 77–75, 75–70, 75–74, 74–70	$6.18 \times 10^{-18}$
10.	69–75, 69–77, 69–47, 69–70, 69–68, 68–81, 68–65, 65–66, 66–49, 49–45, 49–51, 51–52, 51–58	$3.29 \times 10^{-21}$
11.	69–75, 69–70, 70–74, 70–75, 75–77, 77–76, 77–80, 80–81, 80–79, 80–97, 80–96, 96–95, 96–82, 82–83, 82–77	$8.31 \times 10^{-25}$
12.	69–75, 69–68, 69–77, 77–80, 80–79, 80–96, 96–82, 96–97, 96–94, 94–95, 94–100, 100–106, 100–104, 100–103, 100–98, 100–99, 100–92, 92–102, 102–101	$8.91 \times 10^{-36}$

line trappings along with probabilities of cascading failures are given in Tables 2, 3, and 4. A similar explanation holds good for the initial tripping of the lines 37–40, 56–59, and 69–75 depicted in Tables 2, 3, and 4. The probabilities of the major disturbance for the cases given in Tables 2, 3, and 4 are 0.0000526413, 0.001361453, and 0.006955396, respectively.

Furthermore, the simulation of cascading disturbances is carried out with probability ( $p$ ) of individual line incorrect tripping as 0.05. The sample paths and probability for cascading failures for initial tripping of the lines 11–12, 37–40, 56–59, and 69–75 are tabulated in Tables 5, 6, 7, and 8, respectively.

Consider a case of legitimate tripping of the line (11–12) connected between Bus-11 and Bus-12 with incorrect tripping probability ( $p$ ) of 0.05. The sequence of events (sample paths) of tripping of various transmission lines along with the probabilities of a different sequence of tripping events obtained through the simulation is tabulated in Table 5. The probability of the major disturbance initiated with the 11–12 trip can be calculated by summing all the probabilities of sample paths obtained through the simulation studies. For the case shown in Table 5, the probability ‘ $P$ ’ of major disruption has been found to be  $2.76 \times 10^{-6}$  for simulation steps ( $N$ ) of 3000 and  $p = 0.05$ .

A similar kind of simulations is performed with different initiation line tripping (37–40, 56–59, and 69–75 separately) for the same number of iterations and probability of individual line incorrect tripping as above. The sample paths of line trappings along with probabilities of cascading failures are given in Tables 6, 7, and 8. A similar explanation holds good for the initial tripping of the lines 37–40, 56–59, and 69–75 depicted in Tables 6, 7, and 8. The probabilities of the major disturbance for the cases given in Tables 6, 7, and 8 are 0.000007, 0.000001, and 0.00149454, respectively.

In order to understand the overall estimated probabilities of cascading collapse initiated by a single-line tripping in a better way, a bar chart has been plotted as shown in Fig. 9. Figure 9 shows the variation in estimated probabilities of cascading collapse in log scale with different transmission line tripping as the initiating event. From the graph, it is evident that the line connected between Bus-69 and Bus-75 is the most sensitive line in the network, so special care should be taken in protecting this transmission line; otherwise, if the line gets tripped, then the probability of cascading collapse is maximum for this particular case.

## 4.2 Simulation of Cascading Events using Line Power Flow-based Model of Hidden Failure

In this section, similar case studies considered in Sect. 4.1 are conducted with different line tripping (using line power flow-based HF model) as the initiating events. The

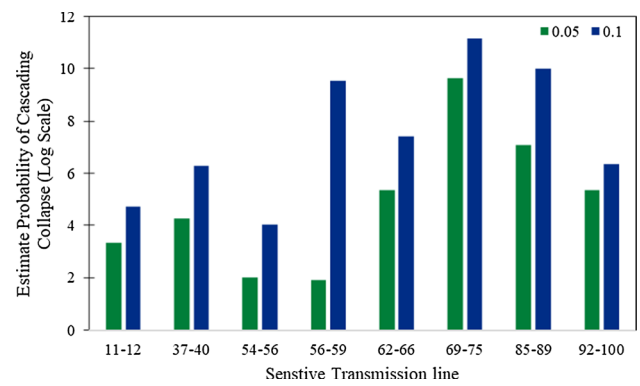


**Fig. 9** Estimated probabilities of cascading collapse for various transmission lines in the IEEE-118 bus system due to HFs of the protection system obtained using impedance-based probability model of HF

**Table 9** Sample paths and probabilities for cascading failures for initial tripping of line 11–12 with  $p = 0.01$

S. no.	Tripped lines	Probability
1.	11–12, 12–117	$6.426 \times 10^{-03}$
2.	11–12, 11–5, 12–117	$1.16 \times 10^{-05}$
3.	11–12, 12–2, 12–117	$5.26 \times 10^{-05}$
4.	11–12, 12–14, 14–15	$1.29 \times 10^{-06}$
5.	11–12, 12–14, 12–117	$5 \times 10^{-06}$
6.	11–12, 12–3, 12–16, 12–117	$2.02 \times 10^{-07}$
7.	11–12, 12–7, 12–14, 12–117	$2.66 \times 10^{-08}$
8.	11–12, 12–16, 12–2, 16–17	$5.7 \times 10^{-08}$
9.	11–12, 12–16, 12–3, 3–1, 3–5	$4.75 \times 10^{-09}$
10.	11–12, 11–4, 12–16, 12–7, 7–6	$1.93 \times 10^{-10}$
11.	11–12, 12–14, 12–3, 12–7, 12–2, 12–117	$4.39 \times 10^{-12}$
12.	11–12, 12–3, 12–14, 12–7, 12–2, 12–117	$4.53 \times 10^{-13}$

corresponding results are tabulated in Tables 9, 10, 11, and 12 for better illustration.

Here also, the first case is considered with the line connected between Bus-11 and Bus-12 tripping legitimately as shown in Fig. 5. The sequence of events (sample paths) of tripping of various transmission lines along with the probabilities of a different sequence of tripping events obtained through the simulation is tabulated in Table 9. The first and second rows in Table 9 show the same sample paths, but the probability values are different. The reason is the difference in tripping sequence; for example, initially the line 11–12 is tripped legitimately. However, in the following steps, either one of the lines 11–12 and 12–117 or both the lines 11–12 and 2–117 have tripped simultaneously resulting in different numerical values of probabilities. The probability of the major disruption initiated with an 11–12 trip can be calculated by summing all the probabilities of sample paths obtained through the simulation studies. For the case shown

**Table 10** Sample paths and probabilities for cascading failures for initial tripping of line 37–40 with  $p=0.01$ 

S. No.	Tripped lines	Probability
1.	37–40, 40–41, 41–42	$6.75729 \times 10^{-05}$
2.	37–40, 37–33, 33–15	$4.04732 \times 10^{-05}$
3.	37–40, 37–33, 33–15	$3.81047 \times 10^{-05}$
4.	37–40, 37–39, 39–40	$3.17989 \times 10^{-05}$
5.	37–40, 40–39, 39–37	$1.60548 \times 10^{-05}$
6.	37–40, 37–35, 35–36	$1.26139 \times 10^{-05}$
7.	37–40, 40–39, 39–37	$5.70204 \times 10^{-06}$
8.	37–40, 37–33, 33–15	$5.42259 \times 10^{-06}$
9.	37–40, 40–39, 39–37	$2.12951 \times 10^{-06}$
10.	37–40, 37–39, 39–40	$1.498 \times 10^{-06}$
11.	37–40, 37–33, 33–15	$9.92097 \times 10^{-07}$
12.	37–40, 40–39, 39–37	$9.92097 \times 10^{-07}$
13.	37–40, 40–42, 40–41	$3.6973 \times 10^{-07}$
14.	37–40, 40–39, 40–41, 41–42	$3.05459 \times 10^{-07}$
15.	37–40, 37–34, 34–36, 36–35	$2.023 \times 10^{-07}$
16.	37–40, 40–41, 40–39, 39–37	$1.24878 \times 10^{-07}$
17.	37–40, 40–42, 42–41, 42–49	$5.93594 \times 10^{-08}$
18.	37–40, 37–34, 37–33, 33–15	$4.95363 \times 10^{-08}$
19.	37–40, 37–34, 37–35, 35–36	$4.0516 \times 10^{-08}$
20.	37–40, 37–34, 34–36, 36–35	$2.26187 \times 10^{-08}$
21.	37–40, 37–35, 37–39, 39–40	$1.09699 \times 10^{-08}$
22.	37–40, 37–35, 37–33, 37–34, 34–19, 19–15, 19–18, 19–20, 34–43	$3.31033 \times 10^{-09}$
23.	37–40, 37–39, 37–35, 37–33, 33–15	$1.1523 \times 10^{-09}$
24.	37–40, 37–33, 37–34, 34–43, 43–44	$6.24186 \times 10^{-10}$
25.	37–40, 37–39, 37–34, 34–36, 36–35	$3.62756 \times 10^{-10}$
26.	37–40, 37–38, 38–30, 30–26, 26–25	$1.05376 \times 10^{-10}$
27.	37–40, 37–38, 37–39, 38–65, 65–64, 65–68, 65–66	$1.78367 \times 10^{-11}$
28.	37–40, 37–38, 37–39, 37–35, 37–33, 33–15	$1.7225 \times 10^{-11}$
29.	37–40, 37–39, 37–34, 34–36, 34–43, 34–19	$7.33855 \times 10^{-13}$
30.	37–40, 37–33, 37–34, 37–39, 37–35, 35–36	$6.77161 \times 10^{-13}$
31.	37–40, 37–38, 37–34, 37–33, 37–35, 37–39	$1.64155 \times 10^{-13}$
32.	37–40, 37–39, 37–34, 37–33, 37–35, 35–36	$9.54014 \times 10^{-14}$
33.	37–40, 37–39, 37–35, 37–34, 37–38, 38–30, 30–8, 8–5, 8–9	$1.90865 \times 10^{-15}$
34.	37–40, 37–39, 37–35, 37–38, 38–65, 65–64, 64–63, 64–61	$6.97889 \times 10^{-17}$
35.	37–40, 37–33, 37–39, 37–35, 37–38, 38–65, 65–64, 65–66, 65–68	$2.25229 \times 10^{-17}$
36.	37–40, 37–33, 37–34, 37–39, 37–38, 38–65, 65–68, 68–81, 81–80	$1.13057 \times 10^{-18}$
37.	37–40, 40–42, 42–49, 49–54, 54–55, 54–59, 59–60, 59–56, 56–55, 55–59	$1.00424 \times 10^{-22}$
38.	37–40, 40–41, 40–42, 42–49, 49–45, 49–51, 49–69, 49–48, 48–46, 49–54	$6.71809 \times 10^{-23}$

in Table 9, the probability of major disruption ( $P_a$ ) is found to be 0.060222626, when the number of simulation steps ' $N$ ' and the probability of individual line incorrect tripping are 3000 and  $p=0.01$ , respectively.

A similar kind of simulations is performed with different initiation line tripping (37–40, 56–59, and 69–75 separately) for the same number of iterations and probability of individual line incorrect tripping as above. The sample paths of line trippings along with probabilities of cascading failures are given in Tables 10, 11, and 12. The above explanation holds good for the initial tripping of

the lines 37–40, 56–59, and 69–75 depicted in Tables 10, 11, and 12. The probabilities of the major disturbance for the cases given in Tables 10, 11, and 12 are 0.000224546,  $2.93901 \times 10^{-05}$ , and  $7.67723 \times 10^{-05}$ , respectively.

Further, the simulation of cascaded disturbances is carried out with probability ( $p$ ) of individual line incorrect tripping as 0.005. The sample paths and probability for cascading failures for initial tripping of the lines 11–12, 37–40, 56–59, and 69–75 are tabulated in Tables 13, 14, 15, and 16, respectively.

**Table 11** Sample paths and probabilities for cascading failures for initial tripping of line 56–59 with  $p=0.01$ 

S. no.	Tripped lines	Probability
1.	56–59, 59–63, 63–64	$2.90488 \times 10^{-05}$
2.	56–59, 59–55, 59–63, 63–64	$2.96387 \times 10^{-07}$
3.	56–59, 56–54, 56–57, 57–50	$3.55537 \times 10^{-08}$
4.	56–59, 56–58, 56–57, 56–54, 56–55	$3.05459 \times 10^{-09}$
5.	56–59, 56–55, 55–54, 54–53, 53–52	$2.70754 \times 10^{-09}$
6.	56–59, 56–55, 55–54, 54–59, 59–55	$1.3 \times 10^{-09}$
7.	56–59, 59–54, 54–49, 49–50, 50–57	$8.7845 \times 10^{-10}$
8.	56–59, 59–54, 59–55, 55–54, 55–56	$5.93594 \times 10^{-10}$
9.	56–59, 59–61, 61–60, 61–62, 61–64	$4.09253 \times 10^{-10}$
10.	56–59, 59–63, 59–61, 61–64, 64–63	$3.85304 \times 10^{-10}$
11.	56–59, 56–55, 56–57, 56–54, 54–53, 56–58	$3.05782 \times 10^{-12}$
12.	56–59, 59–55, 59–63, 59–60, 59–61, 59–54	$4.44457 \times 10^{-14}$
13.	56–59, 59–61, 61–60, 60–62, 61–64, 64–65, 64–63	$2.06626 \times 10^{-14}$
14.	56–59, 56–58, 59–60, 59–55, 59–54, 59–63, 63–64	$4.66868 \times 10^{-15}$
15.	56–59, 59–61, 61–64, 64–65, 65–66, 66–67, 67–62	$3.52354 \times 10^{-15}$
16.	56–59, 59–61, 61–62, 62–67, 62–60, 60–61, 61–64	$9.07258 \times 10^{-16}$
17.	56–59, 59–55, 59–60, 60–61, 61–64, 64–63, 63–59	$2.7713 \times 10^{-16}$
18.	56–59, 59–60, 59–61, 61–64, 64–65, 65–66, 65–38, 65–68	$5.0944 \times 10^{-17}$
19.	56–59, 59–54, 59–60, 59–61, 61–62, 62–66, 62–67, 67–66	$3.15476 \times 10^{-17}$
20.	56–59, 56–57, 56–55, 55–59, 59–54, 59–61, 59–60, 60–61, 60–62	$3.41889 \times 10^{-19}$
21.	56–59, 56–54, 59–55, 59–60, 59–61, 59–54, 54–53, 54–55, 54–49	$2.65928 \times 10^{-19}$
22.	56–59, 56–54, 54–55, 54–49, 55–59, 59–61, 61–64, 64–63, 63–59	$8.05883 \times 10^{-22}$
23.	56–59, 59–60, 59–63, 59–54, 54–55, 54–53, 54–56, 56–57, 57–50	$6.20565 \times 10^{-22}$
24.	56–59, 56–54, 54–49, 49–45, 49–50, 49–47, 49–69, 69–47, 69–68, 69–77, 69–70, 69–75	$2.26907 \times 10^{-25}$
25.	56–59, 56–58, 56–57, 56–54, 54–59, 59–63, 59–60, 60–62, 62–61, 62–66, 62–67	$1.10048 \times 10^{-25}$

Consider the case of legitimate tripping of the line (11–12) connected between Bus-11 and Bus-12 with incorrect tripping probability ( $p$ ) of 0.005. The sequence of events (sample paths) of tripping of various transmission lines along with the probabilities of a different sequence of tripping events obtained through the simulation is tabulated in Table 13. The probability of the major disturbance initiated with the line 11–12 trip can be calculated by summing all the probabilities of sample paths obtained through the simulation studies. For the case shown in Table 13, the probability ‘Pa’ of major disruption has been found to be  $2.76 \times 10^{-6}$  for simulation steps ( $N$ ) of 3000 and  $p=0.005$ .

A similar kind of simulations is performed with different initiation line tripping (37–40, 56–59, and 69–75 separately) for the same number of iterations and probability of individual line incorrect tripping as above. The sample paths of line trippings along with probabilities of cascading failures are given in Tables 14, 15, and 16. A similar explanation holds good for the initial tripping of the lines 37–40, 56–59, and 69–75 depicted in Tables 14, 15, and 16. The probabilities of the major disturbance for the cases given in Tables 14, 15, and 16 are  $0.005650183$ ,  $2.62015 \times 10^{-06}$ , and  $8.42054 \times 10^{-12}$ , respectively.

To have a better understanding of the overall estimated probabilities of cascaded collapse initiated by a single-line tripping, a bar chart has been plotted as shown in Fig. 10. Figure 10 shows the variation in estimated probabilities of cascaded collapse in log scale with different transmission line tripping as the initiating event. Figure 10 shows that the lines connected between Bus-11 and Bus-12, and Bus-85 and Bus-89 are the most sensitive lines in the network, so special care should be taken in protecting this transmission line; otherwise, if the line gets tripped, then the probability of cascaded collapse is maximum for this particular case.

From the discussion carried out in Sects. 4.1 and 4.2, it is clear that the reduction in the individual probability of incorrect line tripping due to HFs of the protection system will reduce the probability of major blackout to a greater extent.

Since the entire study is based on some hypothetical probability models, in order to capture all the possible sample paths (possible sequence of line tripping events leading to blackouts) the value of  $p$  has been changed for different types of model to obtain the best possible results which can include all the sequences. The impedance-based hidden failure model which gave best result with  $p=0.05$  and  $p=0.025$  is chosen to show that reduction in  $p$  can reduce

**Table 12** Sample paths and probabilities for cascading failures for initial tripping of line 69–75 with  $p=0.01$ 

S. no.	Tripped lines	Probability
1.	69–75, 69–68, 68–116	$6.55659 \times 10^{-05}$
2.	69–75, 75–74, 74–70	$1.1069 \times 10^{-05}$
3.	69–75, 69–47, 47–46, 47–49	$4.6171 \times 10^{-08}$
4.	69–75, 69–49, 69–70, 69–77, 69–68, 69–47, 68–65, 68–81, 68–116	$3.21541 \times 10^{-08}$
5.	69–75, 69–70, 70–74, 74–75	$2.00489 \times 10^{-08}$
6.	69–75, 69–77, 69–70, 69–68, 68–116	$1.86659 \times 10^{-08}$
7.	69–75, 69–47, 69–68, 69–70, 69–77, 69–49, 77–75, 77–78, 77–80	$7.96405 \times 10^{-09}$
8.	69–75, 69–70, 69–47, 69–68, 69–77, 69–49, 77–75, 77–78, 77–80	$6.6013 \times 10^{-09}$
9.	69–75, 69–70, 69–47, 69–49, 69–68, 69–77	$2.1555 \times 10^{-09}$
10.	69–75, 75–77, 75–70, 70–74, 74–75	$1.77523 \times 10^{-09}$
11.	69–75, 75–70, 75–118, 75–74, 75–77	$9.14484 \times 10^{-10}$
12.	69–75, 75–74, 75–70, 70–71, 70–74	$8.35397 \times 10^{-10}$
13.	69–75, 75–70, 70–69, 69–68, 68–116	$1.10807 \times 10^{-10}$
14.	69–75, 75–70, 70–69, 70–74, 70–71, 71–73	$2.23689 \times 10^{-11}$
15.	69–75, 75–118, 75–77, 77–76, 76–118	$8.28796 \times 10^{-12}$
16.	69–75, 69–47, 75–74, 75–118, 75–70, 75–77	$1.69001 \times 10^{-12}$
17.	69–75, 75–77, 77–78, 77–82, 82–83, 82–96	$1.69001 \times 10^{-12}$
18.	69–75, 75–77, 77–78, 77–80, 80–79, 80–99, 99–100	$1.72432 \times 10^{-14}$
19.	69–75, 69–68, 69–77, 77–76, 77–75, 77–82, 77–78, 77–80	$4.14263 \times 10^{-18}$
20.	69–75, 75–74, 75–77, 77–78, 77–82, 82–83, 83–85, 82–96	$3.19 \times 10^{-18}$
21.	69–75, 69–47, 69–49, 49–47, 49–50, 49–51, 49–45, 45–46, 45–44	$3.3847 \times 10^{-19}$
22.	69–75, 75–118, 75–70, 75–77, 77–69, 77–82, 82–83, 83–84, 84–85	$3.00015 \times 10^{-19}$
23.	69–75, 69–49, 49–54, 54–59, 54–56, 59–60, 59–56, 56–58, 59–63, 63–64	$1.11926 \times 10^{-20}$
24.	69–75, 75–77, 75–118, 75–70, 70–74, 70–24, 70–69, 69–68, 68–116	$5.96112 \times 10^{-22}$
25.	69–75, 69–47, 69–70, 69–49, 49–54, 49–42, 49–45, 49–51, 51–58, 51–52	$9.88929 \times 10^{-23}$
26.	69–75, 75–70, 75–118, 75–77, 77–76, 77–82, 77–69, 69–49, 49–51, 51–58, 51–52	$1.21426 \times 10^{-24}$
27.	69–75, 69–77, 77–80, 77–76, 77–82, 77–75, 75–70, 70–71, 70–24, 70–69, 69–68, 68–65, 65–38, 65–66, 65–64	$2.28134 \times 10^{-25}$
28.	69–75, 75–118, 75–77, 77–76, 77–80, 80–97, 80–99, 80–98, 80–96, 96–95, 96–94, 96–97	$1.37425 \times 10^{-28}$
29.	69–75, 69–68, 69–70, 69–49, 49–42, 49–45, 49–66, 49–50, 49–48, 49–47, 47–46, 47–69	$2.15542 \times 10^{-29}$
30.	69–75, 75–77, 77–76, 77–78, 77–69, 69–68, 68–81, 68–65, 65–38, 38–37, 37–34, 37–39, 37–33, 33–15	$6.91641 \times 10^{-30}$

**Table 13** Sample paths and probabilities for cascading failures for initial tripping of line 11–12 with  $p=0.005$ 

S. no.	Tripped lines	Probability
1.	11–12, 12–117	$1.703 \times 10^{-03}$
2.	11–12, 12–14, 12–117	$1.28 \times 10^{-05}$
3.	11–12, 11–4, 4–5	$1.14 \times 10^{-06}$
4.	11–12, 12–2, 12–117	$2.94 \times 10^{-06}$
5.	11–12, 12–14, 12–117	$8.3 \times 10^{-06}$
6.	11–12, 12–3, 3–1, 3–5	$5.99 \times 10^{-09}$
7.	11–12, 12–3, 12–7, 7–6	$5.99 \times 10^{-09}$
8.	11–12, 12–7, 12–16, 12–117	$1.98 \times 10^{-10}$
9.	11–12, 12–16, 12–2, 12–117	$2.58 \times 10^{-11}$
10.	11–12, 12–14, 12–2, 12–3, 3–1, 3–5	$5.69 \times 10^{-14}$
11.	1–12, 12–3, 12–16, 12–7, 12–2, 12–14, 14–15	$2.29 \times 10^{-17}$
12.	11–12, 12–14, 12–7, 12–2, 12–3, 3–5, 5–4, 5–11, 11–4	$4.96 \times 10^{-24}$

**Table 14** Sample paths and probabilities for cascading failures for initial tripping of line 37–40 with  $p=0.005$ 

S. no.	Tripped lines	Probability
1.	37–40, 37–35, 35–36	$1.8693 \times 10^{-05}$
2.	37–40, 40–39, 39–37	$3.5395 \times 10^{-06}$
3.	37–40, 37–34, 34–36, 36–35	$1.01965 \times 10^{-08}$
4.	37–40, 40–42, 40–41, 41–42	$9.17773 \times 10^{-09}$
5.	37–40, 40–39, 40–41, 40–42	$8.72903 \times 10^{-09}$
6.	37–40, 40–42, 42–41, 42–49	$7.95057 \times 10^{-10}$
7.	37–40, 37–35, 37–33, 37–39, 39–40	$1.20961 \times 10^{-11}$
8.	37–40, 37–35, 37–33, 37–39, 37–34, 34–19, 19–15, 19–18, 19–20	$2.28296 \times 10^{-13}$
9.	37–40, 37–38, 37–34, 34–43, 34–36, 36–35	$3.12648 \times 10^{-15}$
10.	37–40, 37–38, 37–33, 37–35, 37–39, 39–40	$2.61505 \times 10^{-16}$
11.	37–40, 37–38, 37–33, 37–39, 37–34, 34–36, 34–43, 43–44	$1.36343 \times 10^{-19}$
12.	37–40, 40–42, 42–49, 49–45, 49–54, 49–48, 49–47, 49–50, 49–69, 69–70, 70–24, 24–72, 72–71	$2.55527 \times 10^{-31}$

**Table 15** Sample paths and probabilities for cascading failures for initial tripping of line 56–59 with  $p=0.005$ 

S. no.	Tripped lines	Probability
1.	56–59, 56–58, 58–51	$2.62015 \times 10^{-06}$
2.	56–59, 56–58, 56–55, 56–57, 57–50	$1.47346 \times 10^{-12}$
3.	56–59, 59–63, 59–54, 59–55, 55–54, 55–56	$2.18226 \times 10^{-13}$
4.	56–59, 59–55, 59–61, 59–54, 59–63, 59–60	$1.27231 \times 10^{-14}$
5.	56–59, 59–55, 59–54, 59–61, 59–63, 59–60	$8.22623 \times 10^{-15}$
6.	56–59, 59–54, 59–60, 59–55, 59–63, 59–61	$8.02262 \times 10^{-15}$
7.	56–59, 59–63, 59–55, 55–56, 56–57, 56–58, 58–51	$9.26471 \times 10^{-17}$
8.	56–59, 59–61, 61–60, 60–62, 62–67, 62–61, 62–66	$7.81297 \times 10^{-17}$
9.	56–59, 59–55, 59–63, 59–54, 54–49, 49–66, 49–42, 49–48, 49–51, 49–45, 49–47, 49–50, 49–69	$7.42733 \times 10^{-24}$

**Table 16** Sample paths and probabilities for cascading failures for initial tripping of line 69–75 with  $p=0.005$ 

S. no.	Tripped lines	Probability
1.	69–75, 69–70, 69–77, 69–68, 69–49, 68–116	$8.39056 \times 10^{-12}$
2.	69–75, 75–118, 75–74, 75–70, 70–74	$2.99828 \times 10^{-14}$
3.	69–75, 69–47, 69–70, 70–74, 70–24, 70–71, 71–73	$1.31232 \times 10^{-20}$
4.	69–75, 69–68, 69–77, 77–82, 77–76, 77–80, 80–98, 80–81, 81–68	$1.0065 \times 10^{-23}$
5.	69–75, 69–68, 69–77, 77–76, 77–82, 77–80, 80–96, 80–79, 80–98, 98–100	$3.78694 \times 10^{-24}$
6.	69–75, 75–70, 70–71, 70–69, 69–49, 49–48, 49–50, 49–51, 51–58, 51–52	$4.57533 \times 10^{-26}$
7.	69–75, 69–68, 69–47, 47–49, 49–66, 66–62, 62–61, 62–60, 60–61, 61–64, 64–63, 64–65	$5.10363 \times 10^{-31}$

the overall estimated probability of cascading collapse. Similarly,  $p=0.01$  has been selected for the line power flow-based hidden failure model to obtain the best outcome, and it has been reduced to 0.005 to show a similar decrement in overall estimated probability of major blackout in order to preserve consistency for the results obtained utilizing various models. Thus, relays having self-monitoring and the self-checking facility will have less chance of incorrect tripping due to HFs and lead to less probability of major blackouts.

## 5 Conclusions

This paper presents a detail discussion about hidden failures (HFs) in protection systems and its impact in the power system cascaded disruptions. The study of various modes of HFs has been done successfully. Besides, the probabilistic modeling of HFs has been carried out for simulating the cascaded disruptions in power system occurring due to HFs in protection systems. Further, a



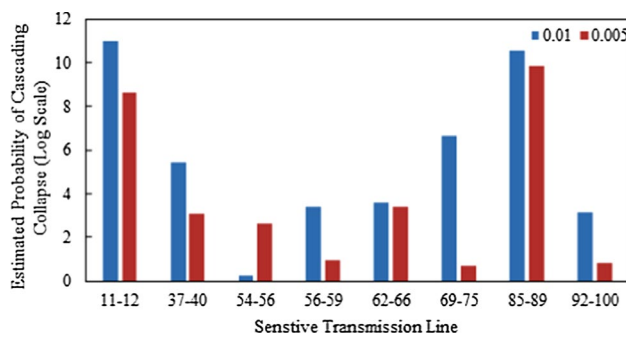


**Fig. 10** Estimated probabilities of cascading collapse for various transmission lines in the IEEE-118 bus system due to HFs of the protection system obtained using power flow-based probability model of HF

methodology has been proposed for investigating the impact of HFs in power system cascaded events through simulation studies conducted in MATLAB software. The results obtained show the efficacy of the proposed methodology. It has been observed that a relay with self-monitoring and self-checking facility can reduce the probability of cascaded disruption to a large extent. Further, the proposed probabilistic analysis and modeling of HFs can help in designing a robust mitigating scheme to prevent cascading events and blackouts.

## References

- Aghamohammadi, M. R., & Salimian, M. R. (2018). A three stages decision tree based intelligent blackout predictor for power systems using brittleness indices. *IEEE Transactions on Smart Grid*, 9(5), 5123–5131.
- Albinali, H. F., & Meliopoulos, A. P. (2017). Hidden failure detection via dynamic state estimation in substation protection systems. In *Saudi Arabia Smart Grid (SASG)*, Jeddah (pp. 1–6).
- Bae, K., & Thorp, J. S. (1999). A stochastic study of hidden failures in power system protection. *Decision Support Systems*, 24(3/4), 259–268.
- Chen, J., Thorp, J., & Dobson, I. (2005). Cascading dynamics and mitigation assessment in power system disturbances via a hidden failure model. *International Journal of Electrical Power Energy System*, 27(4), 318–326.
- Dobson, I., Chen, J., Thorp, J. S., Carreras, B. A., & Newman, D. E. (2002). Examining criticality of blackouts in power system models with cascading events. In *Proceedings of the 35th annual Hawaii international conference on system sciences*, Big Island, HI (pp. 1–10).
- Final Report on the August 14. (2003). Blackout in the United States and Canada: Causes and Recommendations. April 2014. <http://energy.gov/sites/prod/files/oeprprod/DocumentsandMedia/BlackoutFinal-Web.pdf>
- Gao, X., Thorp, J. S., & Hou, D. (2013). Case studies: Designing protection systems that minimize potential hidden failures. In *66th annual conference for protective relay engineers*, College Station, TX (pp. 384–393).
- Henneaux, P. (2015). Probability of failure of overloaded lines in cascading failures. *International Journal of Electrical Power Energy System*, 73(141–148), 2015.
- Horowitz, S. H., Phadke, A. G., & Thorp, J. S. (1995). The role of adaptive protection in mitigating system blackouts. In *1995 CIGRE SC 34 colloquium, Stockholm* (pp. 11–17).
- Hui, R., Xiaozhou, F., Watts, D., & Xingchen, L. (2012). Early warning mechanism for power system large cascading failures. In *IEEE international conference on power system technology (POWERCON)*, Auckland (pp. 1–6).
- Jiao, Z., Gong, H., & Wang, Y. (2018). A D–S evidence theory-based relay protection system hidden failures detection method in smart grid. *IEEE Transactions on Smart Grid*, 9(3), 2118–2126.
- Lai, L. L., Zhang, H., Tian, L., Chun Sing, X., Fang, Y., & Mishra, S. (2013). Investigation on July 2012 Indian blackout. In *2013 international conference on machine learning and cybernetics*, Tianjin (pp. 92–97).
- Li, C., Sun, Y., & Chen, X. (2007). Analysis of the blackout in Europe on November 4, 2006. In *International power engineering conference (IPEC 2007)*, Singapore (pp. 939–944).
- MATLAB and Statistics Toolbox Release. (2014a). The Math Works, Inc., Natick, MA. <https://in.mathworks.com/help/stats/>.
- NERC. (1988). *NERC Disturbance reports 1984–1988*. North American Electric Reliability Council, New Jersey.
- Qi, H., & Shi, L., Sun, Q., & Yao, L. (2016). Risk assessment of cascading failures based on entropy weight method. In *IEEE power and energy society general meeting (PESGM)*, Boston, MA (pp. 1–5).
- Report on Grid Disturbance on 30th July 2012 and Grid Disturbance on 31st July 2012 (2012, August). [http://www.cercind.gov.in/2012/orders/Final\\_Report\\_Grid\\_Disturbance.pdf](http://www.cercind.gov.in/2012/orders/Final_Report_Grid_Disturbance.pdf)
- Seyedi, H., & Sanaye-Pasand, M. (2009). New centralised adaptive load-shedding algorithms to mitigate power system blackouts. *IET Generation, Transmission and Distribution*, 3(1), 99–114.
- Sun, Q., Shi, L., Ni, Y., Si, D., & Zhu, J. (2017). An enhanced cascading failure model integrating data mining technique. *Protection and Control of Modern Power Systems*, 1(1), 1–10.
- Tamronglak, S., Phadke, A. G., Horowitz, S. H., & Thorp, J. S. (1996). Anatomy of power system blackouts: Preventive relaying strategies. *IEEE Transactions on Power Delivery*, 11(2), 708–715.
- Thorp, J. S., Phadke, A. G., Horowitz, S. H., & Tamronglak, S. (1998). Anatomy of power system disturbances: Importance sampling. *International Journal of Electrical Power & Energy*, 20(2), 147–152.
- Wang, X. F., & Xu, J. (2004). Cascading failures in coupled map lattices. *Physical Review E*, 70(1–5), 056113.
- Wu, J. J., Gao, Z. Y., & Sun, H. J. (2006). Cascade and breakdown in scale-free networks with community structure. *Physical Review E*, 74(1–5), 066111.
- Zhao, L., Li, X., Ni, M., Li, T., & Cheng, Y. (2015). Review and prospect of hidden failure: Protection system and security and stability control system. *Journal of Modern Power System and Clean Energy*. <https://doi.org/10.1007/s40565-015-0128-9>.

**Publisher's Note** Springer Nature remains neutral with regard to jurisdictional claims in published maps and institutional affiliations.